Influencing factors of microscanning performance based on flat optical component

Xiubao Sui (隋修宝)*, Lianfa Bai (柏连发), Qian Chen (陈 钱), and Guohua Gu (顾国华)

National Defense Key Laboratory of Optoelectronic Engineering,
Nanjing University of Science and Technology, Nanjing 210094, China
**Corresponding author: sxbhandsome@163.com*

Received November 12, 2010; accepted January 6, 2011; posted online April 18, 2011

To decrease the performance difference between the actual microscanning thermal imager and the theoretical value, a germanium lens (placed at a certain angle between the infrared focal plane array and infrared lens) dip angle model of flat optical component microscanning is introduced in this letter. The model is the basis for choosing the dip angle of the germanium lens, which is used in the microscanning thermal imager. In addition, the actual dip angle of the germanium lens is chosen according to the model, the infrared lens parameters of the thermal imager, and the germanium lens parameters of manufacture and installation. Only in this manner can the optimal performance of the microscanning thermal imager based on the flat optical component be obtained. Results of the experiments confirm the accuracy of the conclusions above.

OCIS codes: 230.3990, 100.6640, 110.4190, 230.4040.
doi: 10.3788/COL201109.052302.

Over the years, improving the spatial resolution of the infrared (IR) images has become an important task in the IR field[1,2], while the optical microscanning technology is an effective way to achieve this goal. In recent years, microscanning technology based on flat optical component (MTFOC) has been rapidly developed; it can break through the following limitations: 1) the detector's filling factor cannot be greater than 100%; and 2) the existing technology, which generates pixel sizes smaller than the diffraction spot sizes, cannot enhance the spatial resolution. Furthermore, MTFOC can address these limitations without changing the pixel sizes of the focal plane array (FPA), the array sizes, and the design of the IR lens[3]. Meanwhile, it can also increase the time utilization of the detector during photoelectric conversion[4,5] and the modulation transfer function of IR images[6]. In actual applications, however, some problems remain; these include the large differences between the actual improved performance of the microscanning thermal imager based on the flat optical component and the theoretical value.

To resolve the problems mentioned above, we conduct the related research based on the germanium lens dip angle model of the flat optical component, and the factors that affect the performance of the microscanning imager. The detailed descriptions are as follows.

The principle diagram of MTFOC is shown in Fig. 1(a), in which incident light L_1 shoots at the germanium lens and L_2 is the exit light. From this figure, we can obtain the following equation[7]:

$$\Delta L = d(1 - \cos i/\sqrt{n^2 - \sin^2 i}), \tag{1}$$

where d is the thickness of the germanium lens, i denotes the incident angle of incident light L_1, n represents the refractive index, and ΔL is the displacement of L_2 to L_1 along the direction of the optical axis.

If L_1 is an adaxial light, the incident angle i is so small that Eq. (1) can be approximately expressed as[7]

$$\Delta L = d(1 - 1/n). \tag{2}$$

If another adaxial light L_1' passes through the flat optical component shown in Fig. 1(b), exit light L_2' intersects with L_2, and then juncture O_1' moves a distance of $d(1 - 1/n)$ relative to O_1 along the optical axis direction. Therefore, when we place a germanium lens at

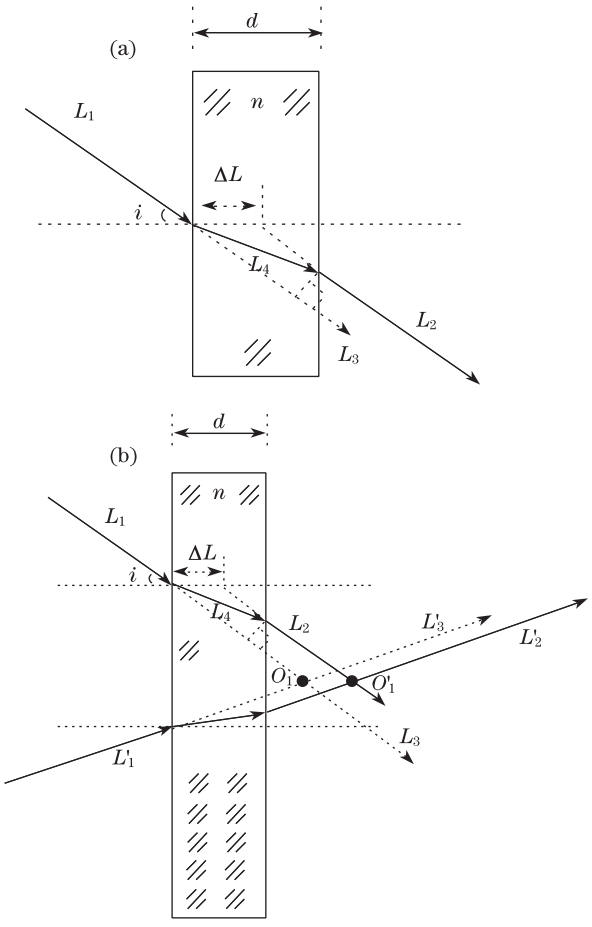

Fig. 1. Schematic of MTFOC.

a certain angle in front of the IRFPA, the IR image of the targets moves a distance of $d(1-1/n)$ along the optical axis direction of the germanium lens. Suppose that the angle between the normal direction of the germanium lens and the normal direction of the FPA is α; considering that all the lights shooting at the FPA are adaxial lights, we can obtain the following equation:

$$d_{||} = \Delta L \times \sin\alpha = d(1-1/n)\sin\alpha, \tag{3}$$

where $d_{||}$ is the displacement of the IR images along the direction parallel to the FPA. Equation (3) is the theoretical basement of MTFOC, and it is limited in that the lights incident to the IRFPA are adaxial.

To evaluate the influencing factors of microscanning, we analyze the 2×2 four-step microscanning mode, which can be easily realized in engineering. The position relationship of the original pixels (no microscanning) and the pixels after microscanning is shown in Fig. 2, in which the blocks filled with white represent the position of the original pixels, and the blocks filled with black represent the position of the pixels after 2×2 four-step microscanning. Suppose the pixel pitch of the detector is d_{pixel}; then, the distance d_{micro} between original pixel O_1 and the nearest scanned pixel m_1 is the $\sqrt{2}d_{\text{pixel}}/4$. To ensure the pixel position relationship of 2×2 four-step microscanning, the position of the scanned pixels reflected by the germanium lens from pixel O_1 can be at m_1 or m_2, and theoretically, even at any blocks filled with black location along the direction of the arrow in Fig. 2. That is, only the equation $d_{||} = (2k+1)d_{\text{micro}}$ should be satisfied in the 2×2 four-step microscanning. Thus, the germanium lens dip angle model of the flat optical components can be expressed as

$$\alpha = \arcsin\frac{(2k+1)\sqrt{2}d_{\text{pixel}}}{4[d(1-1/n)]}\ , k = 0, 1, 2, \cdots. \tag{4}$$

Theoretically speaking, the value k can be chosen randomly according to Eq. (4). The manufacture and installation errors definitely appear when a germanium lens is created and installed in the microscanning devices; meanwhile, the manufacture and installation errors are fixed during a period of time. On one hand, the bigger is the k value, the smaller the influence imposed on the microscanning performance during the installation process, and the better the image quality. On the other hand, upon deriving Eq. (2), we indicate that the prerequisite of the establishment of Eq. (2) is that the lights shooting at the FPA should be adaxial lights. To satisfy this condition, k should be as small as possible. Thus, the final selection of k should be based on the comprehensive consideration of the germanium lens installation, manufacture parameters, and the axis-nearing degree of the lights from the IR lens. Only in this case will the difference between the actual performance and the theoretical value of the microscanning thermal imager be minor.

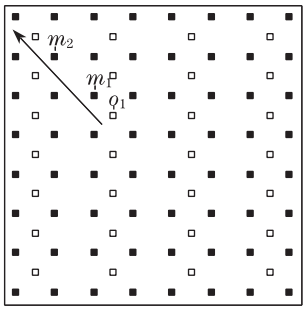

Fig. 2. Location relationship between original pixels and pixels after 2×2 microscanning.

The following examples are actual demonstrations used to verify that different germanium lens dip angles can cause different influences on microscanning performance, and only the installation angle of the germanium lens is optimal in the actual system.

In this example, the 320×240 French-made microbolometer is adopted; the pixel pitch of the detector is 45 μm. Suppose that the thickness of the germanium lens used is 1.5 mm; then, Eq. (4) can be simplified as

$$\alpha = \arcsin[(2k+1)\sqrt{2}\times 10^{-2}]. \tag{5}$$

The relationship between theoretical installation angle α and parameter k is shown in Table 1. The germanium lens is installed on the hypotenuse of the triangle bracket in Fig. 3, in which angle α' is the actual dip angle because of installation error. Suppose that the vertical error caused by the installation and manufacture procedure of the microscanning device is ΔH(to illustrate the problem conveniently, only positive error is considered); we can then obtain

$$\Delta H = H' - H, \tag{6}$$

$$H = L \times \tan\ \alpha_{\text{k}}, \tag{7}$$

$$H' = L \times \tan\ \alpha'_{\text{k}}, \tag{8}$$

then

$$\alpha' = \arctan\frac{L\times\tan\alpha + \Delta H}{L}. \tag{9}$$

Substituting Eq. (9) into Eq. (3), displacement $d'_{||}$ is expressed as

$$d'_{||} = d(1-1/n)\sin\left(\arctan\frac{L\times\tan\ \alpha + \Delta H}{L}\right). \tag{10}$$

The pixel position error is defined as the difference between the theoretical and the actual values. We divide the pixel position error by the theoretical value, and then obtain the ratio

$$\frac{\Delta d_{||}}{d_{||}} = \frac{d'_{||} - d_{||}}{d_{||}} = \frac{\sin\left(\arctan\dfrac{L\times\tan\alpha + \Delta H}{L}\right) - \sin\alpha}{\sin\alpha}. \tag{11}$$

Because the sensitive area of the FPA that we used is 14.4× 10.8 (mm)[8], L is chosen as 30 mm to guarantee that the lens can completely cover the FPA. Meanwhile,

Table 1. Relationship between α and Parameter k when Germanium Lens Thickness is 1.5 mm

k	0	1	2	3
α (deg.)	0.8103	2.4316	4.0548	5.6813

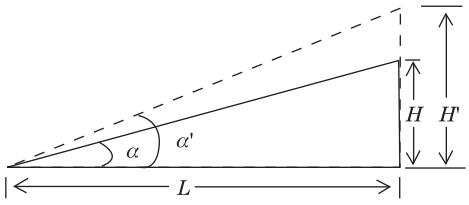

Fig. 3. Schematic of the installation error of germanium lens.

the computer numerical control machining center and the usual vector testing instrument used during the manufacture and installation procedure can both cause an error of 10 μm[9]. Thus, ΔH can be up to 20 μm. The theoretical value of $d_{||}$ and the actual error when k is 0, 1, and 2 are shown in Table 2. The table is based on Eq. (2) which means that the lights from the exit pupil of the IR lens are all considered adaxial. However, in actual systems, a small angle always exists between the lights shooting at the germanium lens and the optical axis of the germanium lens. Suppose that the maximum angle between the lights that participate in imaging and the optical axis of the germanium lens is $i_{\max}$, and the IR lens IR 050 0.8320 ($i_{\max}$ is 30°) manufactured by the Kunming North Optoelectronic Corporation is selected; then, the errors in the microscanning system caused by the non-adaxial lights are shown in Table 3.

According to Table 2, with the increase in k, the installation error parameter becomes larger. According to Table 3, the increase in k generates a smaller microscanning error parameter. Thus, we can conclude that the changing trend of installation error parameter and microscanning error parameter are contrary to each other. With the increase in installation error parameter, microscanning error becomes smaller. The two errors both affect system performance. According to Eq. (10), the system performance is affected by the product of the two errors. The smaller is the product of the two errors, the better the system performance. Therefore, we should select an adaptive k to acquire the best performance. The total error between the theoretical and the actual values of the microscanning system is defined as the product of the germanium lens installation error, manufacture error, and the optical system error. Table 4 shows us the total microscanning error coefficient (MEC) of the microscanning system under different k. The MEC is defined as

$$\mathrm{MEC}=\frac{\cos i/\sqrt{n^2-\sin^2 i}}{1-1/n} \times \frac{\sin(\arctan\frac{L\times\tan\alpha+\Delta H}{L})}{\sin\alpha}. \quad (12)$$

The bigger MEC causes poor performance of the microscanning imager. Table 4 shows that the performance of the microscanning system has the least difference between the actual and the theoretical values when k is 2 from 0 to 3. When k is larger than 3, the total MEC is larger and the performance of the microscanning system gets worse.

To verify the theory mentioned above, we adopt the 320×240 French-made microbolometer, and the parameters of the optical lens are: $F\#$: 1.0; f: 50 mm. The core processor is dm642 (Ti Corporation). The environment temperature is 20 °C. Under these conditions, we obtain four microscanning images when k is from 0 to 3. The images are shown in Fig. 4. From the figures, we can observe that the spatial resolution of Fig. 4(c) is the highest among the four figures and the k value is 2. The spatial resolutions of Figs. 4(b) and (d) are nearly identical and higher than that of Fig. 4(a). Thus, the descending order of spatial resolution is Figs. 4(b), (c), and (d) (the spatial resolution of all figures are the same), and then Fig. 4(a). The experimental results are consistent not only with Table 4, but also with Eq. (12).

According to the experiments above, we can determine that the dip angle of the microscanning germanium lens based on the flat optical components should be selected according to the dip angle model, optical system

Table 2. Installation Error Parameters Corresponding to Different k

k	α(deg.)	α'(deg.)	$d_{\|\|}$(μm)	$d'_{\|\|}$(μm)	$\Delta d_{\|\|}/d_{\|\|}$
0	0.8103	0.8485	15.91	16.66	4.71%
1	2.4316	2.4697	47.73	48.48	1.57%
2	4.0548	4.0928	79.55	80.29	0.93%
3	5.6813	5.7191	111.37	112.11	0.66%

Table 3. Microscanning Error in Accordance with Different $i_{\max}$

$i_{\max}$	$\Delta L/d$	$1-1/n$	$\frac{\cos i/\sqrt{n^2-\sin^2 i}-1/n}{1-1/n}$
30.0000	0.7818	0.75	4.24%
30.6813	0.7832	0.75	4.43%
35.0000	0.7931	0.75	5.75%
36.5000	0.7968	0.75	6.24%

Table 4. Total MEC in Accordance with Different k

k	$\frac{1-\Delta L/d}{1-1/n}$	$\frac{d'_{\|\|}}{d(1-1/n)\times\sin\alpha}$	MEC
0	1.0315	1.0471	1.0800
1	1.0355	1.0157	1.0512
2	1.0397	1.0093	1.0484
3	1.0443	1.0066	1.0512

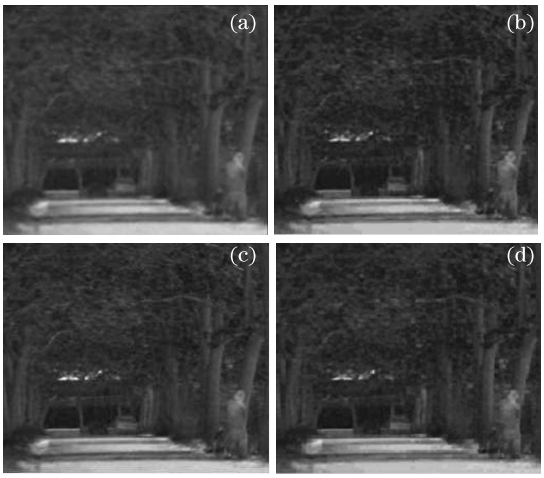

Fig. 4. Microscanning images when (a) k is 0, (b) k is 1, (c) k is 2, and (d) k is 3.

parameters, and the germanium's actual installation and manufacture parameters. To obtain the optimal performance of the microscanning thermal imager, the germanium lens dip angle model must be matched with the installation and manufacture parameters. Thus, the aim to improve the spatial resolution of IR images through microscanning technology can be realized.

This work was supported by the National Defense Pre-Research Fund of China (No. 40405050303), the National Natural Science Foundation of Jiangsu, China (No. BK2008049), and the NUST Research Funding (No. 2010ZDJH12). We appreciate the anonymous reviewer's constructive comments.

References

1. G. Tong and N. Yu, Chin. Opt. Lett. **7,** 465 (2009).
2. L. Zhang, X. Feng, W. Zhang, and X. Liu, Chin. Opt. Lett. **7,** 560 (2009).
3. X. Sui, "Research on the imaging theory and the key techniques of uncooled staring thermal imager", PhD. Thesis (in Chinese) (Nanjing University of Science and Technology, 2009).
4. X. Wang and H. Hua, Opt. Lett. **33,** 449 (2008).
5. X.-B. Sui, Q. Chen, and H.-H. Lu, J. Infrared Millim. Waves (in Chinese) **26,** 377 (2007).
6. X. Wang, J. Zhang, Z. Feng, and H. Chang, Appl. Opt. **44,** 4470 (2005) .
7. X. Li, *Geometrical Optics and Optical Design* (in Chinese) (Zhejiang University Perss, Hangzhou, 1997).
8. 320×240 LWIR uncooled microbolometer detector, Sofradir Corporation (2002).
9. CNC machining center user's guide of GSK218M, CNC Equipment Corporation (2006).